JOURNAL OF THE AMERICAN WATER RESOURCES ASSOCIATION

AMERICAN WATER RESOURCES ASSOCIATION

Spatiotemporal Variability in Water Sources Controls Chemical and Physical Properties of a Semi-arid Urban River System

J.J. Follstad Shah, Y. Jameel, R.M. Smith, R.S. Gabor, P.D. Brooks, and S.R. Weintraub

Research Impact Statement: Mitigation efforts in urban rivers may be better informed by comparing physiochemical patterns (quality) to the relative magnitude of source water inputs (quantity) derived from water isotopes.

ABSTRACT: We conducted synoptic surveys over three seasons in one year to evaluate the variability in water sources and geochemistry of an urban river with complex water infrastructure in the state of Utah. Using stable isotopes of river water ($\delta^{18}O$ and $\delta^{2}H$) within a Bayesian mixing model framework and a separate hydrologic mass balance approach, we quantified both the proportional inputs and magnitude of discharge associated with "natural" (lake, groundwater, and tributary inputs) and "engineered" (effluent and canal inflows) sources. The relative importance of these major contributors to streamflow varied both spatially and seasonally. Spatiotemporal patterns of dissolved oxygen, temperature, pH, calcium, chloride, nitrate, and orthophosphate indicated seasonal shifts in dominant sources of river water played an important role in determining water quality. We show although urban rivers are clearly influenced by novel water sources created by water infrastructure, they continue to reflect the imprint of "natural" water sources, including diffuse groundwater. Resource managers thus may need to account for the quantity of both surface waters and also historically overlooked groundwater inputs to address water quality concerns in urban rivers.

(KEYWORDS: effluent; discharge; hydrology; groundwater; lake; stable isotopes; tributary; water reclamation facility; water quality.)

INTRODUCTION

Urbanization fundamentally alters the hydrologic connectivity of watersheds, with implications for the flow regime and water quality of aquatic ecosystems. Municipalities build infrastructure to divert flow from natural channels to be used for household consumption, industry, and agriculture, as well as to manage stormwater (Pataki et al. 2011; Burns et al. 2012; Fanelli et al. 2017; Locatelli et al. 2017). These hydrologic alterations impact the magnitude of flow in tributaries and recharge to groundwater, which in turn alters the magnitude and timing of flow from these sources to larger rivers. Water used for commercial and domestic purposes often returns to rivers after treatment in a water reclamation facility (WRF) or as untreated irrigation return flow.

While this infrastructure adds complexity to the hydrologic functioning of urban watersheds, it does not fully supplant its natural connectivity (Figure 1) (Gurnell et al. 2007; Brown et al. 2009; O'Driscoll et al. 2010; Ledford and Lautz 2015; Locatelli et al. 2017). In a comparison of cities across the conterminous United

Paper No. JAWRA-18-0025-P of the *Journal of the American Water Resources Association* (JAWRA). Received February 9, 2018; accepted January 15, 2019.

Department of Geography (Follstad Shah), Department of Geology and Geophysics (Jameel, Brooks), and Department of Biology (Smith), University of Utah, Salt Lake City, Utah, USA; School of Environment and Natural Resources (Gabor), The Ohio State University, Columbus, Ohio, USA; and National Ecological Observatory Network (Weintraub), Boulder, Colorado, USA (Correspondence to Follstad Shah: jennifer.shah@envst.utah.edu).

Citation: Follstad Shah, J.J., Y. Jameel, R.M. Smith, R.S. Gabor, P.D. Brooks, and S.R. Weintraub. 2019. "Spatiotemporal Variability in Water Sources Controls Chemical and Physical Properties of a Semi-arid Urban River System." *Journal of the American Water Resources Association* 1–17. https://doi.org/10.1111/1752-1688.12734.

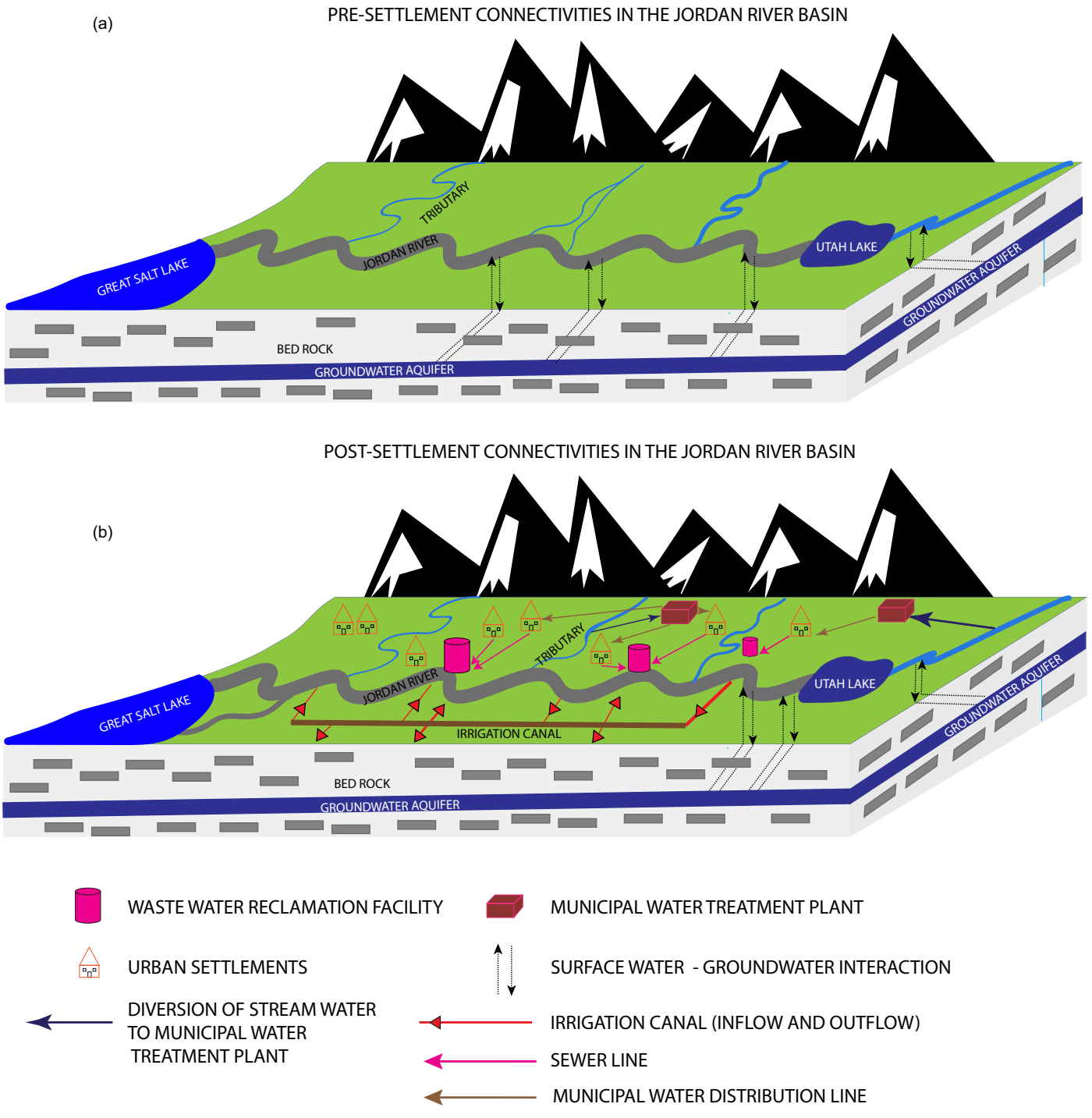

FIGURE 1. Conceptual figure illustrating changes to sources of river water as a result of municipal infrastructure. (a) Pre-settlement condition: river flow originates from upstream surface water, tributary, and groundwater inputs. (b) Post-settlement condition: upstream surface water is managed for crop irrigation, thus augmenting river flow; tributary flow is diverted for municipal and commercial consumption, reducing direct inputs of water to the river; groundwater recharge to river through aquifer is diminished relative to (a); effluent discharge and irrigation canal inflows represent novel inputs of water to the river.

States (U.S.), Hopkins et al. (2015) found heterogeneity in the response of streamflow patterns to urbanization, with climatic and physiographic setting (i.e., slope, permeability) persisting as important predictors of hydrologic parameters. Thus, accurately characterizing the hydro-dynamics of urban rivers requires an understanding of how natural processes, such as groundwater recharge and runoff generation, interact

with water infrastructure to affect both water quantity and quality. The characterization of hydrology and source inputs to urban river systems, and specifically the relative role of natural vs. human-made connectivity, remains a critical step toward sustainable river management.

Many urban rivers have impaired water quality. Identifying targets for remediation requires an understanding of seasonal fluctuations in dominant source waters. The expansion of human water infrastructure and growing water consumption has resulted in a greater number of arid and semi-arid rivers around the world that are now "effluent-dominated" (Brooks et al. 2006). However, there is notable seasonal and spatial variation in the degree to which non-effluent sources interact with wastewater inputs to mediate water quantity and quality. The influence of effluent on water quality can vary in semi-arid rivers (van Vliet et al. 2017), because the effect of wastewater is modulated by the timing and magnitude of dilution potential relative to pollutant concentration (Gurnell et al. 2007; Rice and Westerhoff 2017; Price et al. 2018). Hydrologic flow in some semi-arid urban rivers has been historically snowmelt-dominated, with the greatest potential for dilution occurring in spring when tributary inputs attain annual maximum discharge. Snowmelt also triggers a release of groundwater to surface water in these systems (Becker 2005; Waswa et al. 2013; Kormos et al. 2014a, b; Brooks et al. 2015). Hence, groundwater can be a major source of streamflow for tributaries, as well as for rivers where upwelling occurs.

Groundwater is likely to be higher in quality relative to effluent. However, contaminants can recharge into subsurface aquifers or enter groundwater via subsurface infrastructure, resulting in another source of diminished water quality for urban rivers (Brooks and Lemon 2007; Kaushsal et al. 2011; Hopkins et al. 2015; Hall et al. 2016; Gabor et al. 2017). Moreover, the relative proportion of flow from "natural" water sources may decline in the future as "engineered" inputs (wastewater effluent, untreated canal inflows) increase in response to growing populations and greater volumes of water diverted for human consumption. The degree to which each of these sources influence riverine water quality is dependent on the quality of these sources and their relative contributions to river discharge through time.

Stable isotopes of water can serve as a powerful tool for quantifying the contribution of different water sources to rivers (Baillie et al. 2007; Brooks and Lemon 2007; Bowen et al. 2011; Brooks et al. 2012). Hydrologic processes affect the relative abundance of lighter and heavier isotopes in water molecules through fractionation (Kendall et al. 1995). Isotopic fractionation of water isotopes typically occurs during phase transitions (e.g., liquid to vapor forms). For example, lighter isotopes (^{16}O and ^{1}H) tend toward the vapor phase when water vapor condenses or through evaporation. These processes differentially affect water sources contributing to river discharge (Kendall et al. 1995; Kendall and Caldwell 1998). Analyses of water isotopes have been used in urban watersheds to quantify changes in stormwater discharge resulting from altered stormwater management (Jefferson et al. 2015), to investigate variation in municipal water sources (Ehleringer et al. 2016; Jameel et al. 2016, 2018; Tipple et al. 2017), and to show evidence of interbasin water transfers (Good et al. 2014).

We studied a fourth-order river located in a population center of 1 million people in the semi-arid southwestern U.S. to assess how shifts in dominant source of water influence water quality over an annual cycle. We developed an isotope-based ($\delta^{18}O$ and $\delta^{2}H$) mass balance model and compared it to hydrologic mass balance (HMB) calculations to evaluate seasonal variability in water sources and their magnitude along the Jordan River (Salt Lake City, Utah). We also collected data on physical (water temperature) and chemical (dissolved oxygen [DO] saturation, pH, Cl^{-}, Ca^{2+}, NO_3^{-}, PO_4^{3-}) characteristics to determine whether changes in source waters affected these constituents, which influence aquatic organisms and determine the status of surface water beneficial uses. Our study was partly motivated to inform data gaps identified by an ongoing Total Maximum Daily Load (TMDL) process focused primarily on addressing low DO levels in the river. By quantifying the relative influence of different water sources entering the river, we provide managers with a detailed hydrologic backdrop to work toward attainment of pollutant thresholds.

METHODS

River System

The Jordan River originates at the outlet of Utah Lake (40°53′N 111°58′W; 1,368 m elevation) and flows north, draining into wetlands of the Great Salt Lake (40°21′N 111°53′W; 1,283 m elevation; Figure 2). Roughly 44% of the 2,085 km^2 Jordan River catchment area is urban, with a human population of 1.12 million living in Salt Lake County (U.S. Census Bureau 2016, accessed January 22, 2018). Seven major tributaries drain the Wasatch Mountains and discharge to the river (Figure 2), though several of them are piped underground before doing

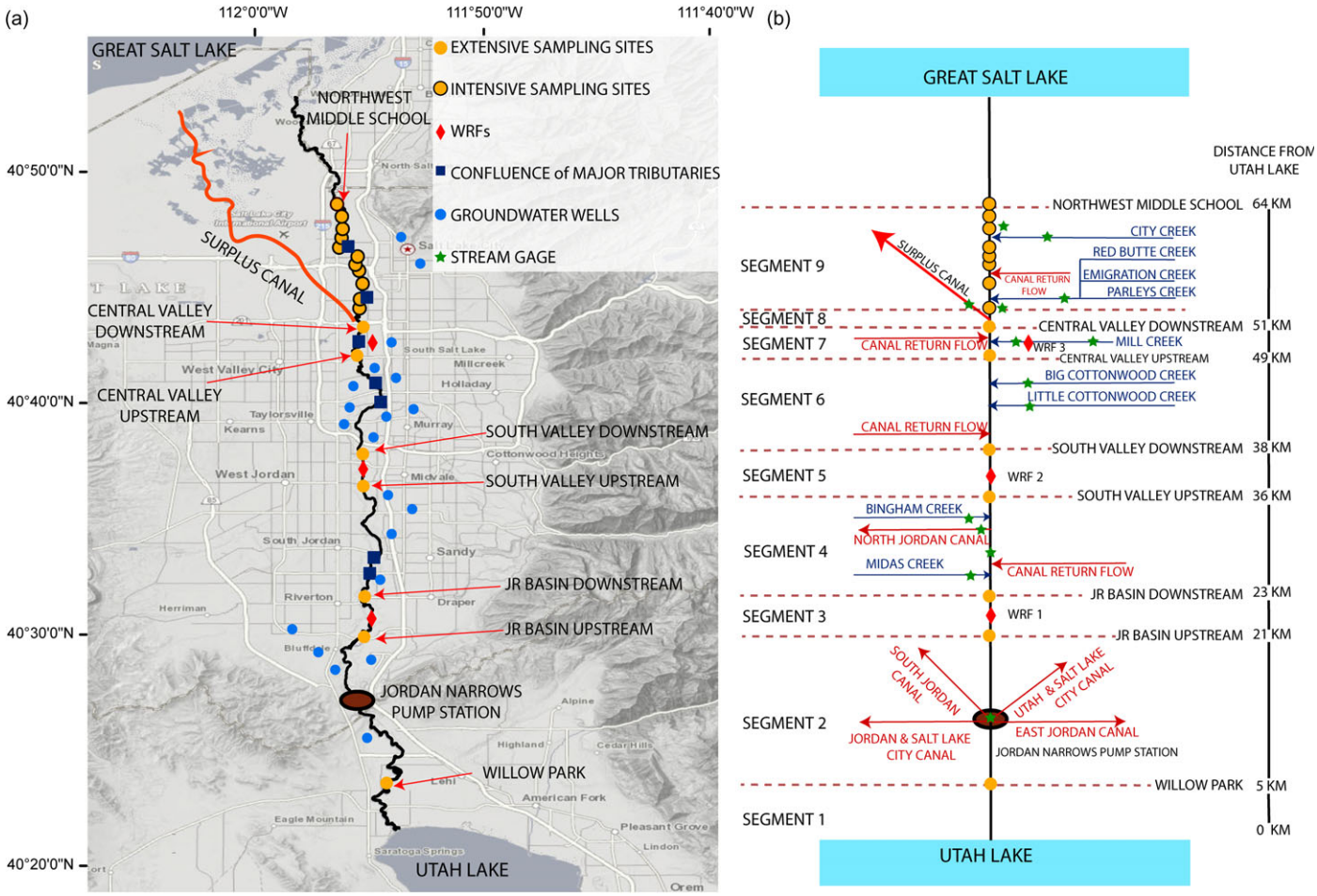

FIGURE 2. (a) Jordan River (black line) flowing through the Salt Lake valley and connecting Utah Lake to the Great Salt Lake. Surplus Canal diverting water from Jordan River to the Great Salt Lake is shown as a red line. Blue circles are the location of groundwater wells to inform groundwater end-member in this study. Blue squares represent the confluence of different tributaries and the Jordan River. Red diamonds are the location of the different water reclamation facilities (WRFs). Orange circles are sampling sites (intensive sites have a black border). Jordan Narrows pump station (brown oval) diverts water from Jordan River to different irrigation canals. (b) Schematic representing nine river segments and source water inputs and outputs within each segment. This schematic was used to inform data parameterization of our Bayesian simple linear mixing (SLM) model.

so. The Jordan River Basin has a cold, semi-arid climate (mean annual air temperature: 12.7°C; mean annual precipitation: 472 mm; U.S. Climate Data 2017, accessed December 1, 2017). Most precipitation falls as snow that feeds the Jordan River in May–June of each year through direct snowmelt runoff and groundwater emergence via the major tributaries. Streamflow is regulated by pumps at Utah Lake and several water diversions. One of these diversions, the Surplus Canal (Figure 2), diverts half of the river flow away from Salt Lake City for flood protection (Epstein et al. 2016). The Jordan River receives water that has interacted with a total of 11 WRFs, four of which are included within our study area. Eight WRFs discharge into Utah Lake, two discharge into the Jordan River itself, and one discharges into a major tributary of the Jordan River (Figure 2). Another WRF located near the Jordan River discharges to a canal draining directly into the Great Salt Lake (not shown).

The Jordan River is listed as impaired under Utah's 303(d) list of impaired water bodies (U.S. Code 1313(d)(1)(A)) in many of its segments, no longer functioning as a cold-water fishery (Jensen and Rees 2005; Epstein et al. 2016). The river is nutrient rich, with mean total nitrogen (N) and total phosphorus (P) concentrations of 4.2 mg N L^{-1} and 0.7 mg P L^{-1}, respectively (Epstein et al. 2016). DO concentrations are episodically hypoxic (<4 mg/L) at locations downstream of the Surplus Canal (Jensen and Rees 2005). Channel morphology is constrained, with widths and depths ranging from 16 to 39 m and from 0.6 to 1.1 m, respectively (Epstein et al. 2016). Slope gradually declines from upstream (0.16%) to downstream

(0.02%) (Epstein et al. 2016), leading to sediment and organic matter accumulation below the Surplus Canal (Jensen and Rees 2005; Epstein et al. 2016).

Study Site Selection, Sampling Design, and Water Sample Collection

We established 18 study sites along the 82 km length of the river (Figure 2), where we conducted field campaigns over three days each in spring (late May), summer (mid-August), and fall (late October) of 2016. These dates were selected to capture seasonal variability in hydrology (high flow in spring and summer, low flow in fall). We selected six study sites within 1 km upstream and 1 km downstream of three effluent discharge locations, as well as one site near the outlet of Utah Lake where the Jordan River originates (Figure 2). Henceforth, we refer to these seven locations as our "extensive" sites. We selected an additional 11 study sites at 1 km intervals along a river reach extending downstream of the Surplus Canal (Figure 2). The distance between these sites was dictated by the experimental design required to assess nutrient transformations in the river, as part of a complementary study (Smith in preparation). Henceforth, we refer to these 11 locations as our "intensive" sites. In addition to these 18 study sites, we also collected water samples from canals at the Jordan Narrows pump station (Figure 2) for analysis of water isotopes from May through October of 2015.

We measured discharge at bridge crossings using a StreamPro Acoustic Doppler Current Meter (ADCP; Teledyne RD Instruments, Poway, California, USA). The ADCP measures integrated velocity of the water column and depth continuously, as an individual on the bridge guides it across the river via an attached rope. After each cross-sectional measurement, StreamPro software is used to calculate channel discharge. We repeated cross-sectional discharge measurements at least three times at each site, until we achieved three replicate discharge measurements within 5% of each other. Discharge values at each site represent the mean of these three measurements. Discharge was measured at all river sites, except at extensive sites in fall 2016 due to equipment failure. We recorded *in situ* water temperature, pH, and DO using a YSI 6920 V2 Sonde (YSI, Yellow Springs, Ohio, USA). All sensors were calibrated before each field campaign.

We collected water samples concurrently with taking sensor measurements. Water isotope samples were collected unfiltered in a glass vial with no headspace and then held at 4°C until analysis. Samples for ion analysis were filtered with a pre-combusted 0.7 μm Whatman GF/F (GE Healthcare Bio-Sciences, Pittsburgh, Pennsylvania, USA) into acid-washed LDPE bottles and frozen until analysis.

Laboratory Analyses

Water isotopes were analyzed within a few weeks of collection at the Stable Isotope Ratios for Environmental Research facility at the University of Utah on a cavity ring-down spectrometer (CRDS) (Picarro L2130-i, Santa Clara, California, USA) following protocols described in Good et al. (2014). Potential biases in the data associated with spectroscopic interferences were identified with ChemCorrect software (Picarro Inc., Santa Clara, California, USA). Accuracy and precision were checked using standard laboratory reference water. The analytical precision for these analyses were $\pm 0.03‰$ for $\delta^{18}O$ and $\pm 0.3‰$ for $\delta^{2}H$ (± 1 standard deviation [SD]). The values are reported in δ notation: $\delta = (R_{sample}/R_{standard} - 1)$, where $R_{sample\ and\ Rstandard}$ are the $^{2}H/^{1}H$ or $^{18}O/^{16}O$ ratios for the sample and standard, respectively, and Vienna Standard Mean Ocean Water (VSMOW) is the standard referenced.

Major anions and cations were measured by ion chromatography on a Metrohm Compact IC (Metrohm, Riverview, Florida, USA). Cation (Ca^{2+}) samples were diluted 8:1. Anion (Cl^{-}, PO_4^{3-}) samples with high concentrations were diluted 6:1 to obtain a linear relationship between peak area and concentration for chloride measurements. Standard curves were calibrated using independent NIST-traceable standards with additional check standards run as unknowns to check analytical precision. We analyzed nitrate and ammonium concentrations using standard colorimetric methods (cadmium reduction with sulfanilamide or hypochlorite with sodium nitroprussides, respectively) on a SmartChem 200 Discrete Analyzer (Westco Scientific, Medford, Massachusetts, USA).

Statistical Analyses

Bayesian Isotope Mixing Model and End-Member Description. We estimated the contribution of different water sources (i.e., Utah Lake, groundwater, tributaries, effluent, and return flow from canals) to the Jordan River through a series of steps. First, we divided the river into nine segments (Figure 2b) that varied with respect to the number of potential sources of water to the river (Table 1). We then calculated the proportional contributions of the different sources at the most downstream location of each segment using a Bayesian simple linear mixing (SLM) model and source values of $\delta^{18}O$ and $\delta^{2}H$, or end-members (Table 1).

We implemented the SLM using the Stable Isotope Mixing Model in R (simmr; Parnell 2016) package in R software (version 3.3.3; R Core Team 2016). The model used a Markov chain Monte Carlo method to

TABLE 1. Isotope values used as end-members for Bayesian SLM modeling and data sources.

Segment	River km	Water source	Spring		Summer		Fall		Data source
			$\delta^{18}O$	$\delta^{2}H$	$\delta^{18}O$	$\delta^{2}H$	$\delta^{18}O$	$\delta^{2}H$	
1	5	Utah Lake	−7.27	−70.71	−2.61	−45.59	−2.61	−45.59	This study
		Groundwater/tributary	−14.03	−110.70	−14.03	−110.70	−14.03	−110.70	Thiros (2003)
2	21	Upstream sources	−7.27	−70.71	−2.61	−45.59	−12.84	−103.91	This study
		Groundwater/tributary	−14.03	−110.70	−14.03	−110.70	−14.03	−110.70	Thiros (2003)
3	23	Upstream sources	−9.56	−84.74	−5.49	−62.27	−11.11	−94.18	This study
		Effluent	−14.42	−110.66	−13.99	−109.25	−14.33	−110.99	This study
4	36	Upstream sources	−11.52	−95.34	−8.17	−77.38	−12.21	−99.77	This study
		Groundwater/tributary	−15.02	−114.22	−15.02	−114.22	−15.02	−114.22	Thiros (2003)
		Midas Creek	−11.24	−94.91	−11.24	−94.91	Dry	Dry	Bowen (2017)
		Bingham Creek	−13.10	−105.13	−13.10	−105.13	Dry	Dry	Bowen (2017)
5	38	Upstream sources	−11.64	−96.31	−8.48	−78.83	−11.99	−99.01	This study
		Canals	−8.17	−77.06	−4.47	−58.13	−4.32	−55.75	This study
		Effluent	−14.70	−112.69	−14.29	−111.06	−14.53	−112.37	This study
6	49	Upstream sources	−12.42	−100.34	−9.70	−86.11	−12.98	−104.01	This study
		Groundwater/tributary	−16.55	122.01	−16.55	122.01	−16.55	122.01	Thiros (2003); Ehleringer et al. (2016); Gabor et al. (2017)
		Canals	−8.17	−77.06	−4.47	−58.13	−4.32	−55.75	This study
7	51	Upstream sources	−14.28	−107.90	−8.28	−77.63	−12.74	−102.60	This study
		Groundwater/tributary	−17.00	−126.30	−17.00	−126.30	−17.00	−126.30	Ehleringer et al. (2016)
		Canals	−8.17	−77.06	−4.47	−58.13	−4.32	−55.75	This study
		Effluent	−15.06	−114.02	−14.87	−113.81	−15.21	−115.85	This study
8	53	Upstream sources	−14.09	−107.07	−9.79	−85.88	−13.77	−108.15	This study
9	64	Upstream sources	−13.70	−105.70	−9.71	−85.42	−13.88	−108.73	This study
		Groundwater/tributary	−16.24	−122.48	−16.24	−122.48	−16.24	−122.48	Thiros (2003); Ehleringer et al. (2016)
		Canals	−8.17	−77.06	−4.47	−58.13	−4.32	−55.75	This study

Note: River kilometer (km) is the most downstream location of each river segment.

estimate the proportional contributions from each water source that would result in the observed riverine isotope values. The model ran thousands of iterations until the proportional contributions converged on a sum of 1. This iterative process provided estimated proportions and associated SDs for water contributions within each river segment. However, the model aggregated contributions from all possible upstream sources into a single category at subsequent downstream locations (Table 1). We parsed these "upstream sources" into different source categories *post hoc* using estimated proportions attributed to each source upstream multiplied by the aggregated proportion for all upstream sources. We then added the product to the estimated proportions for corresponding categories in the downstream segment. These corrections allowed us to assess the cumulative proportion of river flow associated with each water source at all study sites throughout the river's flowpath. We also parsed the SD associated with "upstream sources" to individual sources following the standard uncertainty propagation method (Equation 1):

$$\sum \mathrm{SD}_j^i = \sqrt{(\mathrm{SD}_j^i)^2 + \mathrm{up}_j \times p_{j-1}^i \sqrt{\left(\left(\frac{\mathrm{SD}_{\mathrm{up_j}}}{\mathrm{up}_j}\right)^2\right) + \left(\left(\frac{\mathrm{SD}_{p_{j-1}^i}}{p_{j-1}^i}\right)^2\right)}}, \quad (1)$$

where $\Sigma \mathrm{SD}_j^i$ is the cumulative SD of source (i) at the downstream site of segment (j) (i.e., the error associated with source [i] upstream contributions plus source [i] contributions within segment [j]), SD_j^i is the SD associated with the mean contribution of source (i) in segment (j), up_j is the mean contribution of "upstream sources" at segment (j), $\mathrm{SD}_{\mathrm{up_j}}$ is SD of "upstream sources" at segment (j), p_{j-1}^i is the mean contribution of source (i) in the segment upstream, and $\mathrm{SD}_{p_{j-1}^i}$ is the SD of source (i) in the preceding segment.

We obtained end-member isotope values for sources we did not directly measure (i.e., groundwater and tributaries; Table 1) from published literature (Thiros 2003; Ehleringer et al. 2016; Gabor et al. 2017) and a water isotopes database (Bowen 2017,

accessed August 15, 2017). We averaged reported values for groundwater wells within 1 km of the river within each segment, resulting in one set of groundwater isotope values per segment. We used isotope values from our most upstream study site (Willow Park; Figure 2) as the Utah Lake end-member in spring and summer, as we did not sample that source directly in 2016 and could not find a previously reported value. Observed values at Willow Park in summer also were used as the Utah Lake end-member in fall, given that values at Willow Park in fall were considerably depleted relative to values from summer (see Results and Discussion) and flow from Utah Lake had declined by over 90% as compared to summer discharge rates. Our approach relied on two additional assumptions. First, we assumed a negligible effect of evaporation on governing the isotope values of the river, considering the short length of the river (<80 km) and an average flow rate of more than 3.4 m^3/s. Second, we assumed little to no direct influx of groundwater in Segments 3 and 5 (as opposed to groundwater inputs from upstream), which were 2 km in length and delineated as individual segments due to the presence of a WRF.

HMB Estimation of Water Sources to River. We compared the results of our mixing model to HMB calculations as another means to assess the certainty of water source contributions to the river. In short, we amassed discharge data we collected at our study sites, discharge volumes reported by WRF operators, and reported discharge measured at gaging stations along the river (UTDWR 2018, accessed May 7, 2018; USGS 2017, accessed December 1, 2017) and tributaries (Salt Lake County 2017, accessed December 1, 2017). We compared the discharge we measured at the end of each river segment to the cumulative water inputs from all upstream sources, minus reported water diversions. Hydrologic gaging data for return flow from canals to the Jordan River were unavailable, so these inputs were estimated from imbalances between measured upstream and downstream discharge volumes. HMB calculations were made for spring and summer because we lacked discharge data at some study sites in fall.

Uncertainty in the HMB approach is qualitative due to unknown error associated with discharge measurements reported by other agencies, averaging of some water inputs included in the HMB (e.g., discharge diverted to the Surplus Canal over the two days of sampling each season), and estimation of water inputs calculated by the difference between two locations where discharge was measured (e.g., canal return flows). We considered our HMB calculations to have "low," "moderate," or "high" certainty based on several factors. Water inputs with "low" certainty were not directly measured and comprised river segments for which summed proportions did not equal 1.0. Water inputs with "moderate" certainty were not directly measured but summed proportions within the river segment equaled 1.0. Water inputs with "high" certainty were directly measured and summed proportions within the river segment equaled 1.0.

RESULTS AND DISCUSSION

Dominant Water Sources to the Jordan River Vary Spatially and Temporally

Spatiotemporal patterns in discharge and $\delta^{18}O$ (Figure 3) indicate that dominant water sources to the river vary over an annual cycle. Discharge generally increased through river km 50, ranging 0.9–17.9 m^3/s throughout the study (Figure 3a). Discharge declined by 50% downstream of river km 50 via diversions to the Surplus Canal. Discharge diminished with season, with mean values (and standard errors [SE]) of 5.5 (0.4) m^3/s in spring, 4.6 (1.1) m^3/s in summer, and 3.4 (0.4) m^3/s in fall (Figure 3a). The most pronounced change in discharge occurred in spring downstream of major tributary inputs (Segment 5; Figure 3a), where flow peaked at >17 m^3/s. Following this peak at river km 50, flow rapidly attenuated to <5 m^3/s through the intensive sites by diversion via the Surplus Canal (Segment 8; Figure 3a). Flow remained ≤5 m^3/s at the intensive sites throughout all seasons for urban flood control purposes. Although we did not measure discharge in fall at the upstream extensive sites, we observed a reduction of ~1 m in surface water elevation, concomitant with a 92% reduction of Utah Lake inputs from summer (3.66 m^3/s) to fall (0.28 m^3/s), as recorded at the Jordan Narrows pump station.

Mean (and SE) $\delta^{18}O$ values were enriched in summer ($-9.1 \pm 0.5‰$) relative to spring ($-12.9 \pm 0.4‰$) and fall ($-13.3 \pm 0.2‰$). Enriched values of $\delta^{18}O$ at our upstream study site (Willow Park) location in spring and summer were likely the result of water inputs from Utah Lake, which should be enriched in $\delta^{18}O$ due to high rates of evaporation (Fuhriman et al. 1981; Gat 1996; Brooks et al. 2014). Indeed, sampling of both Utah Lake water and water from Willow Park in spring of 2018 showed that the two locations had identical $\delta^{18}O$ values ($-7.6‰$). In addition, $\delta^{18}O$ values we observed in 2018 were very similar to the values we observed at Willow Park in spring 2016 ($-7.3‰$) and more depleted with respect to the values we observed at Willow Park in summer 2016 ($-2.2‰$, Table 1). Canal inflows to the river also

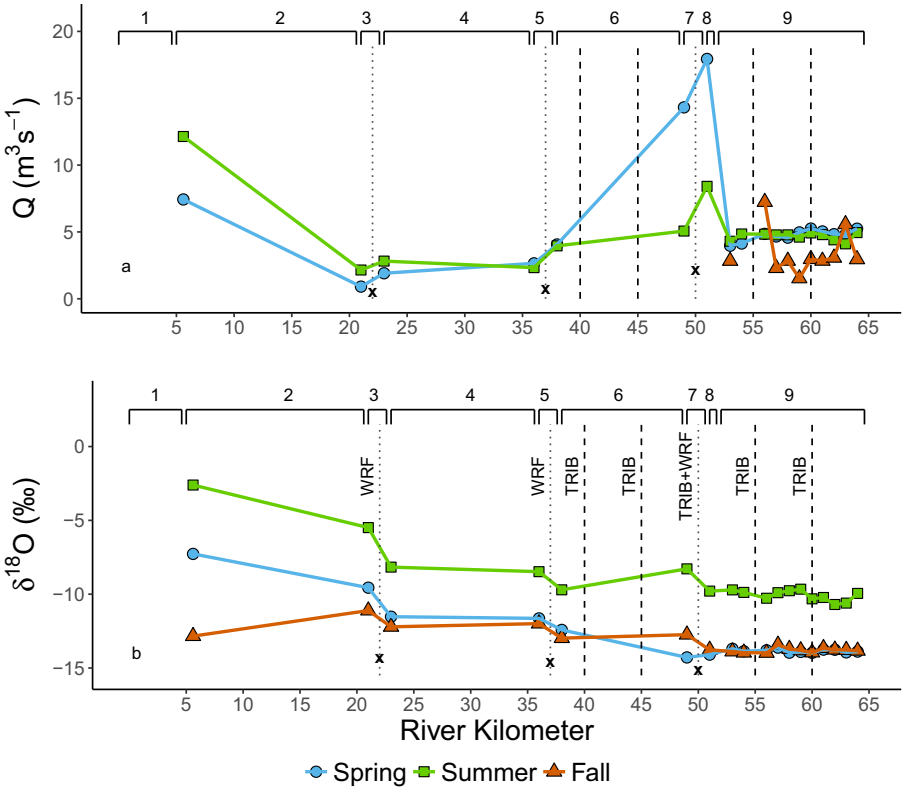

FIGURE 3. Discharge (m^3/s, a) and water column $\delta^{18}O$ (‰, b) vary with distance downstream (km) and across three seasons. Dashed vertical lines indicate locations of tributary inputs along the river flowpath and dotted vertical lines denote effluent outfall locations. "X" denotes mean discharge of effluent or mean concentration of each constituent in effluent averaged across three seasons. Brackets indicate river Segments 1–9, as illustrated in Figure 2.

have enriched $\delta^{18}O$ values (−4.2‰ to −9.0‰; Table 1), relative to more depleted groundwater and tributary inputs (−11.0‰ to −17.5‰; Table 1).

$\delta^{18}O$ values of groundwater and tributary inputs were indistinguishable because groundwater can contribute to surface water flow in tributaries (Becker 2005; Waswa et al. 2013; Kormos et al. 2014a, b; Brooks et al. 2015) and evaporation effects are not significant with respect to tributaries of the Jordan River and groundwater (Ehleringer et al. 2016). Groundwater has low seasonal isotopic variability in groundwater relative to surface water (Kendall and Coplen 2001; Gibson et al. 2005; Landwehr et al. 2014). Seasonal variation in groundwater isotope values is attenuated as water moves through soil into aquifers (Clark and Fritz 1997). Consequently, long-term groundwater datasets have shown little variation in groundwater isotope values (Krabbenhoft et al. 1990; Engelhardt et al. 2014), including studies conducted in the Salt Lake Valley over a 24-year period (1991–2015) (Thiros and Manning 2004; Jameel et al. 2016). These studies suggest that our application of averaged groundwater $\delta^{18}O$ values within each river segment to our SLM is reasonable.

$\delta^{18}O$ values of effluent overlap with groundwater and tributaries to some extent, ranging from −14.0‰ to −15.2‰ in our study (Figure 3b; Table 1). We observed the most depleted values of $\delta^{18}O$ in spring at the same location where discharge attained its peak level (river km 49), indicating that tributary inflows depleted in $\delta^{18}O$ can influence the $\delta^{18}O$ signature of the mainstem. This pattern has been documented in other mountainous catchments, such as the Willamette River basin (Brooks et al. 2012), where mixing of snowmelt-fed creek and groundwater contributes to isotopic depletion proportional to inflow volume.

We used both $\delta^{18}O$ and $\delta^{2}H$ values (Table 2) to increase the precision of the SLM. The values of $\delta^{18}O$ and $\delta^{2}H$ we observed co-vary and adhere to the regional meteoric water line described by Ehleringer et al. (2016). Hence, riverine spatiotemporal patterns of $\delta^{2}H$ values were similar to those observed for in $\delta^{18}O$ values and are not more fully described herein.

The SLM and the HMB analyses provided further evidence that the dominant sources of water to the river differ at distinct locations and times of year (Figure 4; Table 2). The certainty of the estimates for both approaches was highest in the upper reach (above river km 36), which has fewer water sources

TABLE 2. Proportional inputs of water from different sources in three seasons estimated through a Bayesian SLM model and a hydrologic mass balance (HMB) approach.

			SLM			HMB		Model difference	
Segment	**River km**	**Source**	**Spring (SD)**	**Summer (SD)**	**Fall (SD)**	**Spring**	**Summer**	**Spring**	**Summer**
1	5	Utah Lake	1.00 (0.000)	1.00 (0.000)	0.12 (0.003)	1.00**	1.00**	0.00	0.00
		Groundwater/tributary	0.00 (0.000)	0.00 (0.000)	0.88 (0.003)	NA	NA	NA	NA
2	21	Utah Lake	0.65 (0.003)	0.74 (0.002)	0.10 (0.004)	0.64***	0.74***	0.01	0.00
		Groundwater/tributary	0.35 (0.004)	0.26 (0.003)	0.90 (0.005)	0.36***	0.26***	−0.01	0.00
3	23	Utah Lake	0.38 (0.04)	0.51 (0.03)	0.07 (0.02)	0.45**	0.57**	−0.07	−0.06
		Groundwater/tributary	0.21 (0.02)	0.18 (0.03)	0.60 (0.02)	0.26**	0.19**	−0.05	−0.01
		Effluent	0.41 (0.06)	0.31 (0.04)	0.33 (0.09)	0.29***	0.24***	0.12	0.07
4	36	Utah Lake	0.25 (0.08)	0.49 (0.04)	0.05 (0.07)	0.14**	0.32**	0.11	0.17
		Groundwater/tributary	0.47 (0.18)	0.19 (0.03)	0.71 (0.19)	0.20*	0.19*	0.27	0.00
		Effluent	0.27 (0.08)	0.31 (0.04)	0.24 (0.09)	0.21***	0.29***	0.06	0.02
5	38	Utah Lake	0.12 (0.05)	0.18 (0.09)	0.01 (0.03)	0.09*	0.19*	0.03	−0.01
		Groundwater/tributary	0.22 (0.09)	0.07 (0.03)	0.22 (0.10)	0.13*	0.11*	0.09	−0.04
		Effluent	0.52 (0.14)	0.49 (0.09)	0.69 (0.10)	0.27**	0.29**	0.25	0.20
		Canals	0.15 (0.09)	0.26 (0.11)	0.08 (0.03)	0.13*	0.20*	0.02	0.06
6	49	Utah Lake	0.05 (0.04)	0.07 (0.06)	0.01 (0.02)	0.03**	0.15**	0.02	−0.08
		Groundwater/tributary	0.53 (0.30)	0.16 (0.18)	0.34 (0.26)	0.83**	0.33**	−0.30	−0.17
		Effluent	0.22 (0.15)	0.21 (0.15)	0.50 (0.25)	0.08**	0.23**	0.14	−0.02
		Canals	0.21 (0.16)	0.56 (0.18)	0.15 (0.10)	0.07*	0.29*	0.14	0.27
7	51	Utah Lake	0.03 (0.03)	0.03 (0.03)	0.00 (0.008)	0.02**	0.09**	0.01	−0.06
		Groundwater/tributary	0.47 (0.23)	0.20 (0.11)	0.33 (0.18)	0.71*	0.34*	−0.24	−0.14
		Effluent	0.26 (0.13)	0.28 (0.11)	0.51 (0.25)	0.19**	0.39**	0.07	−0.11
		Canals	0.24 (0.12)	0.49 (0.20)	0.15 (0.06)	0.08*	0.18*	0.16	0.31
8	53	Utah Lake	0.03 (0.03)	0.03 (0.03)	0.00 (0.008)	0.02**	0.09**	0.01	−0.06
		Groundwater/tributary	0.47 (0.23)	0.20 (0.11)	0.33 (0.18)	0.71*	0.34*	−0.24	−0.14
		Effluent	0.26 (0.13)	0.28 (0.11)	0.51 (0.25)	0.19**	0.39**	0.07	−0.11
		Canals	0.24 (0.12)	0.49 (0.20)	0.15 (0.06)	0.08*	0.18*	0.16	0.31
9	64	Utah Lake	0.03 (0.02)	0.02 (0.02)	0.00 (0.005)	0.02**	0.08**	0.01	−0.06
		Groundwater/tributary	0.52 (0.19)	0.28 (0.11)	0.51 (0.24)	0.73**	0.34**	−0.21	−0.06
		Effluent	0.19 (0.10)	0.20 (0.09)	0.31 (0.19)	0.16**	0.34**	0.03	−0.14
		Canals	0.27 (0.10)	0.50 (0.18)	0.18 (0.08)	0.09*	0.25*	0.18	0.25

Note: River kilometer (km) is the most downstream location of each river segment. Proportions reflect cumulative source water contributions (i.e., contributions from all sources upstream and within the identified segment). Discharge was not available for some sites in fall, so the HMB shows data only for spring and summer. Model difference indicates concordance between model estimates, as calculated by SLM minus HMB values. SD refers to the standard deviation of the SLM estimate. Asterisks indicate confidence of the HMB estimate, where * represents low certainty, ** represents moderate certainty, and *** represents high certainty (see text for criteria upon which these categories are based).

(2–3, depending on segment). Estimates of groundwater inputs were relatively certain between river km 0–23, given the availability of discharge flow rates from Utah Lake and effluent in this segment. Hence, the two approaches found high agreement in source water proportional inputs through river km 23 (Table 2). Uncertainty increased downstream due to the increasing number of water sources and greater potential for inaccuracies as proportional inputs and error of estimates is propagated throughout the flowpath. Nonetheless, the two approaches agreed, with ≤10% difference in estimates, in 57% of cases (Table 2). Differences in estimates >20% occurred in only 17% of cases (Table 2). On average, estimates from the two approaches differed by 11% in spring and 10% in summer.

Comparisons between the estimates derived from the SLM and HMB helped to minimize uncertainty in some instances and identify areas where uncertainty remained high. For example, groundwater inputs at river km 5 (Segment 1) could only be quantified through the SLM. Water isotopes ($\delta^{18}O$ and $\delta^{2}H$) collected from Utah Lake and the river at river km 5 were identical in spring (see Bayesian Isotope Model and End-Member Description), indicating that water in the river comes almost entirely from the lake at this time or has inadequate groundwater inputs to result in depletion of isotopic values. In contrast, water isotope values at river km 5 in fall, when Utah Lake outflow has been largely shut down, strongly reflect groundwater signatures (Table 1). The HMB approach informed interpretation of SLM estimates of groundwater plus tributary inputs between river km 49–64 with high uncertainty. Here, tributary inputs were gaged. Hence, the HMB indicated that the SLM underestimated inputs from groundwater plus tributaries in Segments 4 and 6. However, measured discharge from tributaries was within the margin of error associated

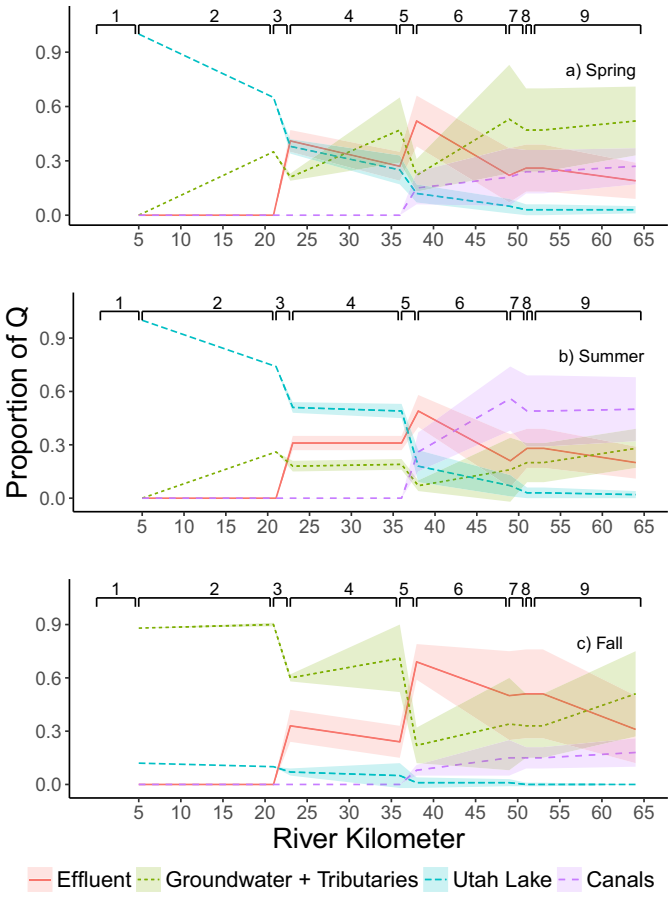

FIGURE 4. Proportion of river water attributed to different sources along the flowpath across three seasons (a, spring; b, summer; c, fall), as estimated by a Bayesian SLM model using water isotopes (δ^{18}O and δ^{2}H) for each source. Shading represents the SD of the estimated proportion for each water source within individual river segments (Table 2). Groundwater and tributary sources are combined because their isotopic signatures were indistinguishable. Brackets indicate river Segments 1–9, as illustrated in Figure 2.

with the SD of the SLM estimates in both segments. Comparison of the results from both approaches aided explanation of uncertainty at river km 38. Here, well-quantified measures of effluent discharge showed that the SLM overestimated the contribution of effluent to the river. However, it is possible that this overestimation was due to poor mixing of water between the effluent outfall location and our study site. The two models largely agreed with respect to contributions from all other water sources at river km 38, but high certainty of SLM estimates for these sources provided greater confidence in HMB estimates. Uncertainty in HMB estimates stemmed from poorly quantified discharge measures for groundwater, tributaries, and canals and the assumption that a diversion upstream of river km 38 diverted water from all sources in equal proportion. Despite the uncertainty associated with both the SLM and HMB, concurrence in over half of the comparisons between the two approaches is notable, suggesting that these dual methods to quantify source water contributions to the river yield reasonable approximations. We use SLM estimates in our remaining results and discussion regarding spatiotemporal variation in source water inputs because the error of the estimates was better quantified relative to the error attributed to HMB estimates.

Results of our SLM model show that estimates of the proportion of river flow attributed to each water source (Table 2; Figure 4) confirm general patterns revealed by variation in discharge and δ^{18}O values with river kilometer (Figure 3). In spring, inputs from Utah Lake dominated flow through river km 21 (>65%), declined to 25%–38% of flow between river km 23–36, and represented the lowest fraction of flow (3%–12%) after river km 38 (Figure 4a; Table 2). This pattern mirrored the observed depletion of δ^{18}O values (by 7‰) between our most upstream and downstream study site locations (Figure 3b). Groundwater represented 21%–35% of flow through river km 21, after which it was augmented by flow from tributaries. Together, groundwater and tributary inputs contributed 22%–53% of flow as of river km 36. HMB calculations indicated these inputs came almost entirely from tributaries as of river km 49. In summer (Figure 4b; Table 2), water from Utah Lake was the dominant contributor of flow to the river upstream of km 36 (49%–74%), but was surpassed by effluent inputs (49%) at river km 38. However, effluent contributions quickly declined to 20%–28% of flow downstream, with increased canal inputs that represented 50% of flow between river km 49–64. Groundwater contributed slightly less to flow upstream of river kilometer 21 (≤26%), as compared to spring. Downstream, combined groundwater and tributary inputs provided ≤25% of flow. Similar to spring, a consistent depletion in δ^{18}O values was observed throughout the flowpath in summer as contributions from Utah Lake diminished. However, δ^{18}O values were consistently enriched in summer as compared to other seasons due to greater outflow from Utah Lake (12.14 m^3/s in summer vs. 7.43 m^3/s in spring) and less runoff from major tributaries in river Segments 6–9 concomitant with major contributions from canal return flows. In fall (Figure 4c; Table 2), water from Utah Lake diminished to 5%–12% of flow upstream of river km 38, in contrast to much higher spring and summer contributions. Combined groundwater and tributary inputs became the greatest contributor to flow through river km 36 (>60%), as well as downstream of river km 53 (51%). However, no tributary inputs occurred prior to river km 23, while they exceeded groundwater inputs downstream of river km 53. A shift toward groundwater as the primary water source between river km 0–21 resulted in more depleted riverine δ^{18}O values, as compared to other seasons. Less flow from Utah Lake and

tributaries in fall relative to other seasons allowed effluent to dominate flow between river km 38–53 (50%–69%). Canals contributed ≤25% of flow between river km 49–64 in both spring and fall.

Our results indicate that dominant water sources were different in the reaches above and below river kilometer ~38, regardless of season. In addition, dominant sources for each river segment shifted over an annual cycle. Contributions to river flow from Utah Lake were still evident at our farthest downstream study site (river km 64) in spring and summer (Figure 5; Table 2), albeit at a very low percentage (3%). The direct input of groundwater to the Jordan River occurs predominantly upstream of river km 36 (UTDWQ 2012). Groundwater inputs contribute 8%–10% of discharge in river Segments 1–4 on an annual basis (UTDWQ 2012, this study), but may exceed 50% of flow in fall (Table 2). Groundwater contributions downstream of river km 36 are masked by tributary inputs in Figures 4 and 5, but represent 1%–2% of measured discharge up to river km 51 in spring and summer and through river km 64 in fall. Taken together, the results of our mixing model suggest hydrologic connectivity between the river and natural water sources (groundwater and tributaries) is ongoing and persistent, although urban water sources (effluent, canal inputs) often dominate flow. Hence, river management must continue to take into consideration both natural and urban sources as influences upon river hydrology, while recognizing the spatial and temporal variation associated with these water sources.

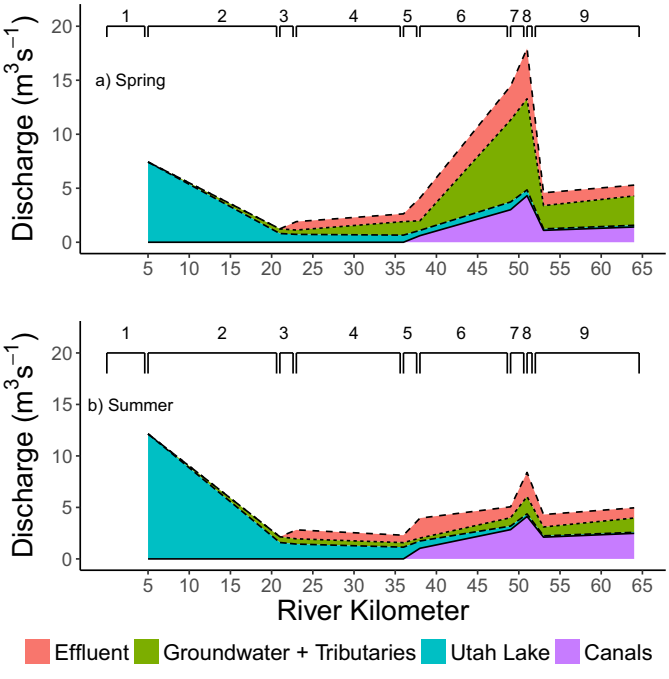

FIGURE 5. Discharge (m^3/s) attributed to different sources along the flowpath in spring (a) and summer (b). Proportional inputs were not applied to discharge in fall due to missing discharge data at some study sites. Brackets indicate river Segments 1–9, as illustrated in Figure 2.

Estimates of discharge associated with different water sources in spring and summer (Figure 5) revealed that the magnitude of flow originating from these sources varied with season. In spring (Figure 5a), effluent inputs augmented discharge in both the upstream and downstream reaches of the river, but sharp increases in flow in the downstream reach (below river km 36) resulted primarily from tributary and canal inputs. In summer (Figure 5b), a greater magnitude of flow in the upstream reach (above river km 36) originated from Utah Lake as compared to flow patterns in spring. River discharge was still greater downstream vs. upstream in summer, as attenuated tributary inputs were offset by an increased magnitude of canal inflows. These seasonal changes in discharge from different water sources were surprising given that contributions from some sources were similar, on a proportional basis (Table 2). For example, contributions from Utah Lake (3%) were similar in spring and summer (Table 2); yet, discharge volumes differed by roughly 50% between the two seasons (0.54 m^3/s in spring, 0.25 m^3/s in summer). We also can compare effluent inputs relative to total discharge in spring vs. fall, although we lack hydrologic measures for all study sites in fall. Cumulative inputs from effluent discharged from the three WRFs were similar in both spring and fall (~3.4 m^3/s). However, these inputs represented 19% and 63% of flow just downstream of the third WRF (river km 51) in spring and fall, respectively. These results suggest it is important to assess the relative magnitude of flows from various sources in addition to relative proportions, since variable loads of constituents within water (e.g., pollutants) can be transported to the river from these different sources.

In summary, both field measures and modeling indicated that dominant sources of water to the river vary over an annual cycle, with contributions from both "urban" and "natural" sources representing major inputs at specific locations and in different seasons. These emergent patterns of variation are logical, given the existing spatial configuration of the lake, tributaries, and water infrastructure within the catchment, predictable seasonal snowmelt runoff, and known river regulation regimes. However, and surprisingly, we found that source water inputs primarily occurring upstream (i.e., lake inputs and groundwater exchange) were evident tens of kilometers downstream, even when inputs were initially low relative to other sources. This result is particularly striking for groundwater inputs, which we likely underestimated due to our inability to isolate groundwater contributions from concurrent tributary contributions. We argue that our approach is beneficial because it quantifies when and

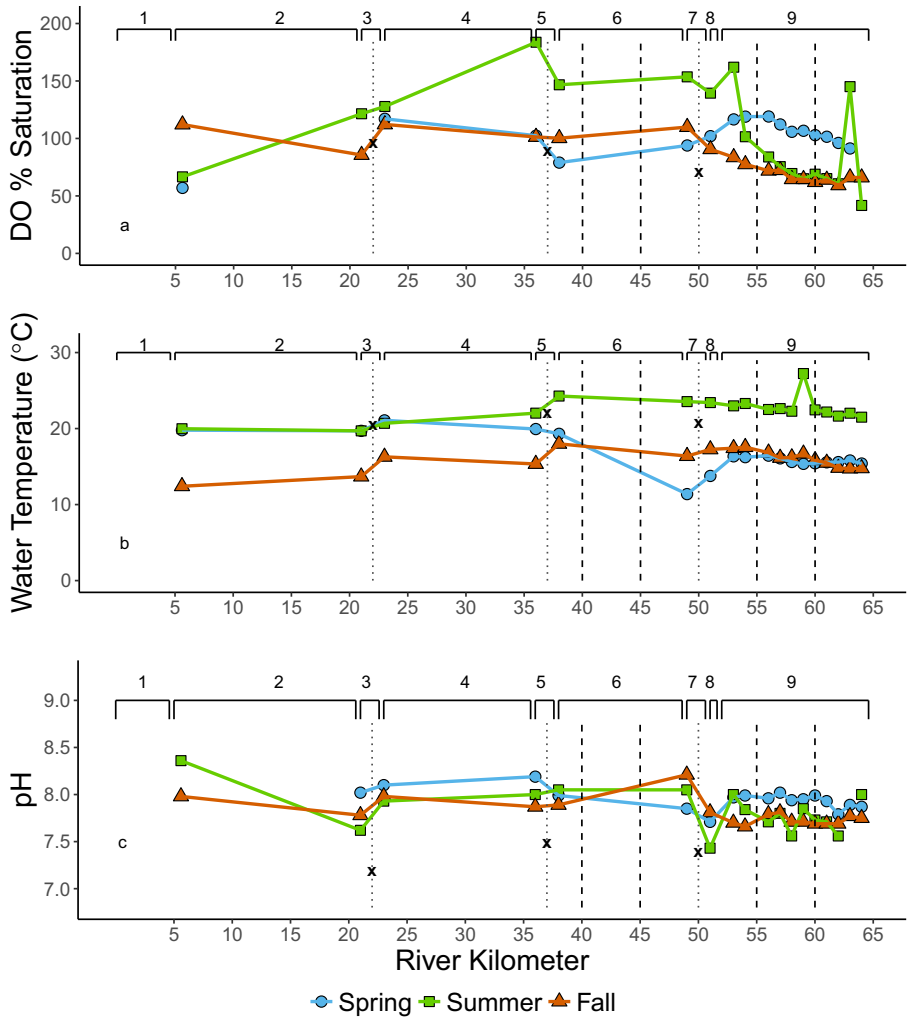

FIGURE 6. Dissolved oxygen (% saturation, a), water temperature (°C, b), and pH (c) with distance downstream across three seasons. Dashed vertical lines indicate locations of tributary inputs along the river flowpath and dotted vertical lines denote effluent outfall locations. "X" denotes mean concentration of each constituent in effluent averaged across three seasons. Brackets indicate river Segments 1–9, as illustrated in Figure 2.

where major shifts in source waters occur. In addition, water isotopes can be measured with relative ease and lower cost compared to metering of all water inputs. Finally, consequences of source water inputs, including constituent loads, can be better assessed with information on both the relative proportion and magnitude of these inputs. We provide further evidence for this point by linking source water contributions to patterns of hydrochemistry within the Jordan River.

Variation in Dominant Water Sources Influences Hydrochemistry

We observed significant seasonal and spatial variation in the physicochemical properties of the Jordan River. Spatiotemporal patterns of DO, temperature, and pH corresponded to change in source water inputs through space and time (Figure 6). DO ranged from 41.7% to 183.7% saturation, with seasonal mean values (and SE) of 101.4 (4.0) % saturation in spring, 104.3 (10.2) % saturation in summer, and 81.3 (4.4) % saturation in fall (Figure 6a). Greatest super-saturation (>100%) of DO occurred in summer, the season of peak autotroph activity. Spatial variability in DO saturation was most evident in summer, with a steady increase between river km 5–51, then a sharp decline in values in Segment 9 (downstream of the Surplus Canal diversion). These trends are consistent with previous reports of net autotrophy upstream of the Surplus Canal and net heterotrophy downstream of this location (Epstein et al. 2016). Spatiotemporal change in DO saturation was associated with shifts in water sources, in addition to differences in productivity between reaches. For example, DO saturation declined by 30% from summer to fall at river km 21 (Figure 6a),

coinciding with a 64% decline in inputs of water from Utah Lake and a concomitant increase in groundwater inputs of the same magnitude (Table 2). In addition, DO saturation increased in all seasons between river km 38–49 (Figure 6a), coincident with water inputs from tributaries. However, the magnitude of increase in DO saturation (4%–16%) was less than the increase in water inputs from tributaries (12%–31%) between river km 38–49.

Water temperature ranged from 11.4°C to 27.2°C, with seasonal mean values of 16.6 (0.6) °C in spring, 22.5 (0.4) °C in summer, and 15.9 (0.3) °C in fall (Figure 6b). Water temperature was most variable in spring, when the lowest temperature was recorded downstream of the first two major tributary inputs to the river that had been draining snowmelt runoff. Tributary inputs maintained similarly cool water temperatures in spring and fall at the intensive study sites. Water temperatures in the upstream reach were similar in spring and summer presumably due to the dominance of Utah Lake inputs in these seasons, while a 30% decline in water temperatures in fall at river km 21 reflected an increase in groundwater inputs. Water temperature was most elevated in summer relative to other seasons between river km 38–64 concomitant with major contributions of relatively warm water from effluent, canal, and tributary inputs. Effluent water temperature is approximately 20°C (Figure 6b), with little variation seasonally. Water in canals was presumably warmer due to absorption of high inputs of solar radiation into low volume drainage systems, while water temperature of tributaries in summer also is roughly 20°C (Gabor et al. 2017; USGS 2017).

pH ranged from 6.00 to 8.36, with seasonal mean values of 7.95 (0.03) in spring, 7.73 (0.11) in summer, and 7.81 (0.03) in fall (Figure 6c). No consistent seasonal trend existed with respect to pH along the river's flowpath, but pH was more dynamic downstream of the Surplus Canal relative to upstream. Effluent discharge also was more acidic relative to river pH.

We observed notable spatiotemporal variation of anions and cations associated with changing water sources (Figure 7). Though Cl^- and Ca^{2+} are considered conservative elements, they still proved to be dynamic in the Jordan River. Cl^- ranged from 93.4 to 337.5 mg/L, with seasonal mean values of 135.6 (4.3) mg/L in spring, 211.8 (9.3) mg/L in summer, and 136.1 (7.5) mg/L in fall (Figure 7a). Ca^{2+} ranged from 42.2 to 94.5 mg/L, with seasonal mean values of 59.3 (3.1) mg/L in spring, 74.0 (2.1) mg/L in summer, and 55.3 (1.8) mg/L in fall (Figure 7b).

Evaporation from Utah Lake may explain why we observed elevated Cl^- concentrations in the river at our most upstream study site in all seasons. Cl^- concentrations declined by 38% from summer to fall at river km 21, coincident with opposing, large shifts in Utah Lake and groundwater inputs to the river. High inputs from canals in summer, which also are subject to evaporative effects, may have maintained the elevated Cl^- concentrations we observed throughout the downstream reach (river km 38–64; Figure 7a). Dilution from groundwater and tributaries also affected Cl^- dynamics. Cl^- concentrations declined by 27% in spring between river km 38–49, in concert with a 31% increase in groundwater and tributary inputs (Figure 7a). Other declines in Cl^- concentrations were evident just downstream of tributary inputs at river km 60 in both spring and summer.

In contrast, we observed low Ca^{2+} concentrations in our most upstream study location, where Utah Lake is the dominant water source (Figure 7b). Ca^{2+} concentration generally increased downstream of the first effluent outfall, reaching its maximum at river km 38 in all seasons, perhaps due to mixing of water through this broad, shallow upstream reach (relative to the downstream reach) with substrate rich in calcium carbonates. This explanation is supported by inconsistent effects on Ca^{2+} concentrations downstream of effluent inputs between river km 21–38 (Figure 7b). Elevated Ca^{2+} concentrations persisted in summer relative to other seasons downstream of river km 38, possibly due to canal inputs rich in calcium-based fertilizers. Like Cl^-, lowest Ca^{2+} concentrations occurred in spring at river km 49 (47% decline relative to river km 38), just downstream of major tributary (31% increase) inputs.

Variation in reactive nutrients (NO_3^- and PO_4^{3-}) was associated with effluent, tributary, and canal inputs. NO_3-N ranged from below detection to 9.9 mg/L, with seasonal mean values of 2.0 (0.2) mg/L in spring, 4.4 (0.3) mg/L in summer, and 5.6 (0.6) mg/L in fall (Figure 7c). PO_4^{3-} ranged from below detection to 0.58 (0.11) mg/L, with seasonal mean values of 0.11 (0.02) mg/L in spring, 0.28 (0.04) mg/L in summer, and 0.29 (0.05) mg/L in fall (Figure 7d). Clear increases in NO_3-N and PO_4-P concentrations occurred downstream of effluent discharge points (Figure 7c,7d). The magnitude of increases in these nutrients downstream of WRFs was greater than the volume of water sourced to the river from effluent, reflective of the high concentration of nutrients observed in effluent (Figure 7c,7d). Dilution by tributary inputs likely resulted in the low concentrations (relative to other sites rather than absolute value) we observed for both nutrients in spring at river km 49. This declining trend downstream of tributary inputs at river km 49 was evident for PO_4-P in all seasons. Elevated concentrations of both NO_3-N and PO_4-P between river km 53–64 in summer may be the result of high canal inputs replete with nutrient-rich fertilizers. Although canal inputs declined from summer to fall, they still may have

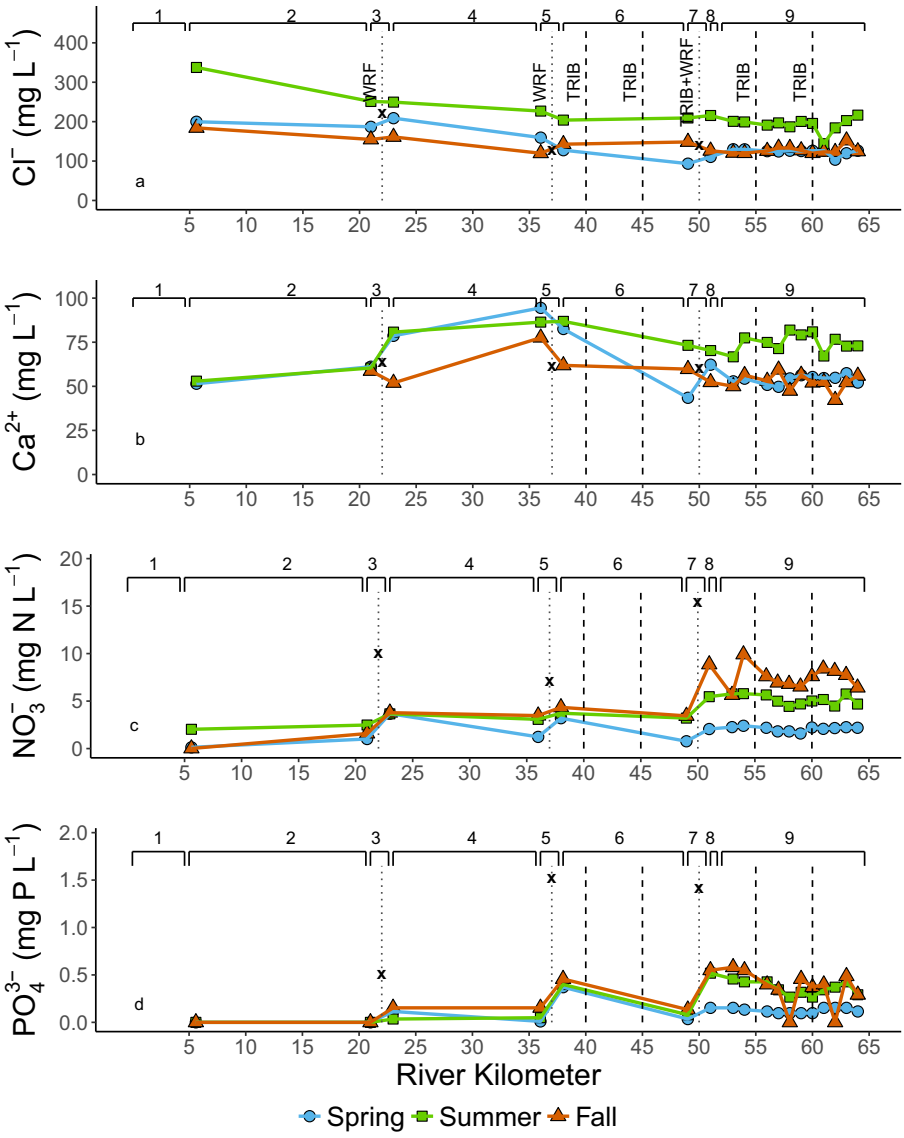

FIGURE 7. Variation in (b) cation (Ca^{2+}) and (a, c–d) anion (Cl^-, NO_3^-, PO_4^{3-}) concentrations (mg/L) with distance downstream across three seasons. For (c) NO_3^- and (d) PO_4^{3-}, concentrations are in mg/L N or P. Dashed vertical lines indicate locations of tributary inputs along the river flowpath and dotted vertical lines denote effluent outfall locations. "X" denotes mean concentration of each constituent in effluent averaged across three seasons. Brackets indicate river Segments 1–9, as illustrated in Figure 2.

contributed to the high nutrient concentrations we observed in fall due to lower overall streamflow.

Implications for Water Resource Management

Spatiotemporal variation in the physiochemistry of urban river systems is common. However, this variation can be problematic when key parameters (e.g., DO or nutrients) exceed regulatory thresholds. Our results show that characterizing shifts in water sources along an urban river flowpath can help to elucidate variation in physiochemical parameters that influence the growth and reproduction of aquatic organisms (Paul and Meyer 2001) and contribute to the status of surface water beneficial uses. Understanding the relative influence of multiple water sources on key physiochemical parameters may help managers prioritize strategies for mitigating impairment.

An example from the Jordan River is illustrative. Low DO % saturation between river km 53–64 in summer and fall can partly be attributed to large diversions of water via the Surplus Canal. Such diversions can slow water velocity in addition to reducing streamflow, resulting in organic matter and sediment accumulation. This pattern was less evident in spring due to elevated tributary inputs that can augment DO. We showed that water temperature

and nutrient concentrations in river Segment 9 are elevated in summer and fall relative to spring and other study site locations (Figures 6b and 7c,7d). Warmer water generally favors net consumption of oxygen in streams, through increased rates of respiration relative to production (Demars et al. 2016; Song et al. 2018). Higher nutrient availability can stimulate both processes in some systems, but is dependent on other factors as well, such as light availability and flow regime (Bernhardt et al. 2017). We attributed elevated temperature in summer to inputs from effluent, canals, and tributaries. However, effluent inputs were the primary source of nutrients to the river, given that their nutrient concentrations were often an order of magnitude greater than the river (Figure 7c,7d) and they were a major water source in summer and fall (Figures 4 and 5). As a result, effluent nutrient loads represented the majority of total riverine nutrient loads (Smith in preparation). Elevated tributary inputs in spring consisting of comparatively lower nutrient concentrations (<3 mg/L N; Gabor et al. 2017) helped to mitigate high nutrient loads from effluent through dilution, as seen in other studies. These tributary inputs include an important fraction of water from groundwater springs with concentrations of Cl^- and NO_3^- indicative of urban impacts (Gabor et al. 2017). Thus, groundwater contributions to the river can occur directly through channel upwelling or indirectly through tributary inflows comprised of newly sourced water from aquifers. The presence of polluted groundwater also suggests that continued efforts to mitigate nonpoint pollutant sources must occur in tandem with nutrient reduction from point sources.

Water resource managers involved in the ongoing TMDL process are considering flow augmentation and nutrient reduction measures to manage low DO conditions that prevent the Jordan River from being removed from Utah's 303(d) list of impaired water bodies. Our results suggest flow augmentation is most critical in fall, when water levels are lowest and nutrient concentrations are high, but they may also help to reduce water temperature in summer. In addition, nutrient reduction efforts may have the greatest effect on riverine nutrient loads in summer and fall.

CONCLUSIONS

Our study used water stable isotopes within a mixing model approach, HMB calculations, and synoptic sampling to better understand urban river hydrology and its effect on water quality. Our analyses indicate that "natural" water sources (inputs from lakes, tributaries, and groundwater) are evident throughout the length of a highly modified urban river and remain major contributors of flow at distinct locations and times of year, though "urban" inputs (effluent, canal inflows) are indeed dominant during certain seasons and at locations where flow is artificially low for flood control. Although lake and tributary inputs are the dominant source of "natural" water inputs to the Jordan River, diffuse groundwater inputs are at times of similar magnitude, on a proportional basis, to inputs from both lakes and tributaries. Improved ability to distinguish between groundwater and tributary inputs using measures of stable isotopes and conservative tracers would be a major advancement, especially since these measures are easier to obtain relative to direct groundwater exchange measurements. The shifting dominance of different source water inputs is reflected in the variation of physical and chemical parameters, suggesting that our approach can be used to better identify sources that degrade surface water quality at specific times or locations along the river continuum. Effects on water quality from lake, effluent, and tributary inputs were apparent in our study, while a more nuanced influence of groundwater may persist through differences in water temperature, control of nutrient cycling, and retention at the sediment–water interface and hyporheic exchange (Dahm et al. 1998), or inputs of contaminated groundwater (Navarro and Carbonell 2007). Given that groundwater can be a significant contributor of river discharge via direct inputs and tributary flow, resource managers must consider its role in the provisioning of water or maintenance of high-quality surface water, in addition to more evident "urban" sources, such as effluent.

ACKNOWLEDGMENTS

The authors gratefully acknowledge the four WRF operators who provided data and access to facilities. Alexander Anderson, Dr. Jeff Horsburgh, and Dr. Beth Neilson loaned equipment. Dr. Suvankar Chakraborty provided analytical insights and Michael Navidomskis assisted with field sampling and laboratory analysis. Funding was provided by EF-0120142 and EPS 1208732 from the U.S. National Science Foundation, as well as grants from the Jordan River Farmington Bay Water Quality Council and the University of Utah Undergraduate Research Opportunities Program. Three anonymous reviewers provided comments that greatly improved the manuscript.

LITERATURE CITED

Baillie, M.N., J.F. Hogan, B. Ekwurzel, A.K. Wahi, and C.J. Eastoe. 2007. "Quantifying Water Sources to a Semiarid Riparian Ecosystem, San Pedro River, Arizona." *Journal of Geophysical Research* 112: G03S02. https://doi.org/10.1029/2006jg000263.

Becker, A. 2005. "Runoff Processes in Mountain Headwater Catchments: Recent Understanding and Research Challenges." In *Global Change and Mountain Regions: Advances in Global Change Research* (Volume 23), edited by U.M. Huber, H.K.M. Bugmann, and M.A. Reasoner, 283–95. Dordrecht: Springer. https://doi.org/10.1007/1-4020-3508-x_29.

Bernhardt, E.S., J.B. Heffernan, N.B. Grimm, E.H. Stanley, J.W. Harvey, M. Arriota, A.P. Appling et al. 2017. "The Metabolic Regimes of Flowing Waters." *Limnology and Oceanography* 63 (S1): S99–118. https://doi.org/10.1002/lno.10726.

Bowen, G. 2017. "Waterisotopes Database." http://waterisotopes.org.

Bowen, G.J., C.D. Kennedy, Z. Lui, and J. Stalker. 2011. "Water Balance Model for Mean Annual Hydrogen and Oxygen Isotope Distributions in Surface Waters of the Contiguous United States." *Journal of Geophysical Research: Biogeosciences* 116 (G4): 1–14. https://doi.org/10.1029/2010JG001581.

Brooks, B.W., T.M. Riley, and R.D. Taylor. 2006. "Water Quality of Effluent-Dominated Ecosystems: Ecotoxicological, Hydrological, and Management Considerations." *Hydrobiologia* 556: 365–79. https://doi.org/10.1890/ES11-00338.1.

Brooks, J.R., J.J. Gibson, S.J. Birks, M.H. Weber, K.D. Rodecap, and J.L. Stoddard. 2014. "Stable Isotope Estimates of Evaporation: Inflow and Water Residence Time for Lakes across the United States as a Tool for National Lake Water Quality Assessments." *Limnology & Oceanography* 59 (6): 2150–65. https://doi.org/10.4319/lo.2014.59.6.2150.

Brooks, J.R., P.J. Wigington, D.L. Phillips, R. Comeleo, and R. Coulombe. 2012. "Willamette River Basin Surface Water Isoscape ($\delta^{18}O$ and $\delta^{2}H$): Temporal Changes of Source Water within the River." *Ecosphere* 3 (5): 1–21. https://doi.org/10.1890/es11-00338.1.

Brooks, P.D., J. Chorover, Y. Fan, S.E. Godsey, R.M. Maxwell, J.P. McNamara, and C. Tague. 2015. "Hydrological Partitioning in the Critical Zone: Recent Advances and Opportunities for Developing Transferable Understanding of Water Cycle Dynamics." *Water Resources Research* 51: 1–15. https://doi.org/10.1002/2015WR017039.

Brooks, P.D., and M.M. Lemon. 2007. "Spatial Variability in Dissolved Organic Matter and Inorganic Nitrogen Concentrations in a Semiarid Stream, San Pedro River, Arizona." *Journal of Geophysical Research: Biogeosciences* 112 (3): 1–11. https://doi.org/10.1029/2006JG000262.

Brown, L.R., T.F. Cuffney, J.F. Coles, F. Fitzpatrick, G. McMahon, J. Steuer, A.H. Bell, and J.T. May. 2009. "Urban Streams across the USA: Lessons Learned from Studies in 9 Metropolitan Areas." *Journal of the North American Benthological Society* 28 (4): 1051–69. https://doi.org/10.1899/08-153.1.

Burns, M.J., T.D. Fletcher, C.J. Walsh, A.R. Ladson, and B.E. Hatt. 2012. "Hydrologic Shortcomings of Conventional Urban Stormwater Management and Opportunities for Reform." *Landscape and Urban Planning* 105: 230–40. https://doi.org/10.1016/j.landurbplan.2011.12.012.

Clark, I.D., and P. Fritz. 1997. *Environmental Isotopes in Hydrogeology* (First Edition). Boca Raton, FL: CRC Press.

Dahm, C.N., N.B. Grimm, P. Marmonier, H.M. Valett, and P. Vervier. 1998. ""Nutrient Dynamics at the Interface between Surface Waters and Groundwaters." *Freshwater Biology* 40 (3): 427–51. https://doi.org/10.1046/j.1365-2427.1998.00367.x.

Demars, B.O.L., G.M. Gíslason, J.S. Ólafsson, J.R. Manson, N. Friberg, J.M. Hood, J.J.D. Thompson, and T.E. Freitag. 2016. "Impact of Warming on CO_2 Emissions from Streams Countered by Aquatic Photosynthesis." *Nature Geoscience* 9: 758–63. https://doi.org/10.1038/NGEO2807.

Ehleringer, J.R., J.E. Barnette, Y. Jameel, B.J. Tipple, and G.J. Bowen. 2016. "Urban Water — A New Frontier in Isotope Hydrology." *Isotopes in Environmental and Health Studies* 52: 477–86. https://doi.org/10.1080/10256016.2016.1171217.

Engelhardt, I., J.A.C. Barth, R. Bol, M. Schulz, T.A. Ternes, C. Schüth, and R. Van Geldern. 2014. "Quantification of Long-Term Wastewater Fluxes at the Surface Water/Groundwater-Interface: An Integrative Model Perspective Using Stable Isotopes and Acesulfame." *Science of the Total Environment* 466: 16–25. https://doi.org/10.1016/j.scitotenv.2013.06.092.

Epstein, D.M., J. Kelso, and M.A. Baker. 2016. "Beyond the Urban Stream Syndrome: Organic Matter Budget for Diagnosis and Restoration of an Impaired Urban River System." *Urban Ecosystems* 19: 1623–43. https://doi.org/10.1007/s11252-016-0556-y.

Fanelli, R., K. Prestegaard, and M. Palmer. 2017. "Evaluation of Infiltration-Based Stormwater Management to Restore Hydrological Processes in Urban Headwater Streams." *Hydrological Processes* 31: 3306–19. https://doi.org/10.1002/hyp.11266.

Fuhriman, D.K., B.M. Lavere, A.W. Miller, and H.S. Stock. 1981. "Hydrology and Water Quality of Utah Lake." *Great Basin Naturalist Memoirs* 5: 43–67.

Gabor, R.S., S.J. Hall, D.P. Eiriksson, Y. Jameel, M. Millington, T. Stout, M.L. Barnes et al. 2017. "Persistent Urban Influence on Surface Water Quality via Impacted Groundwater." *Environmental Science and Technology* 51 (17): 9477–87. https://doi.org/doi.org.10.1021/acs.est.7b00271.

Gat, J. 1996. "Oxygen and Hydrogen Isotopes in the Hydrologic Cycle." *Annual Review of Earth and Planetary Science* 24 (1): 225–62. https://doi.org/10.1146/annurev.earth.24.1.225.

Gibson, J.J., T.W.D. Edwards, S.J. Birks, N.A. St Amour, W.M. Buhay, P. MacEachern, B.B. Wolfe, and D.L. Peters. 2005. "Progress in Isotope Tracer Hydrology in Canada." *Hydrological Processes* 19 (1): 303–27. https://doi.org/10.1002/hyp.5766.

Good, S.P., C.D. Kennedy, J.C. Stalker, L.A. Chesson, L.O. Valenzuela, M.M. Beasley, J.R. Ehleringer, and G.J. Bowen. 2014. "Patterns of Local and Nonlocal Water Resource Use across the Western U.S. Determined via Stable Isotope Intercomparisons." *Water Resources Research* 50: 8034–49. https://doi.org/10.1002/2014WR015884.

Gurnell, A., M. Lee, and C. Souch. 2007. "Urban Rivers: Hydrology, Geomorphology, Ecology and Opportunities for Change." *Geography Compass* 1 (5): 1118–37. https://doi.org/10.1111/j.1749-8198.2007.00058.x.

Hall, S.J., S.R. Weintraub, D. Eiriksson, P.D. Brooks, M.A. Baker, G.J. Bowen, and D.R. Bowling. 2016. "Stream Nitrogen Inputs Reflect Groundwater across a Snowmelt-Dominated Montane to Urban Watershed." *Environmental Science and Technology* 50 (3): 1137–46. https://doi.org/10.1021/acs.est.5b04805.

Hopkins, K.G., N.B. Morse, D.J. Bain, N.D. Bettez, N.B. Grimm, J.L. Morse, M.M. Palta, W.D. Shuster, A.R. Bratt, and A.K. Suchy. 2015. "Assessment of Regional Variation in Streamflow Responses to Urbanization and the Persistence of Physiography." *Environmental Science and Technology* 49 (5): 2724–32. https://doi.org/10.1021/es505389y.

Jameel, Y., S. Brewer, R.P. Fiorella, B.J. Tipple, S. Terry, and G.J. Bowen. 2018. "Isotopic Reconnaissance of Urban Water Supply System Dynamics." *Hydrology and Earth System Sciences* 22: 1–17. https://doi.org/10.5194/hess-22-1-2018.

Jameel, Y., S. Brewer, S.P. Good, B.J. Tipple, J.R. Ehleringer, and G.J. Bowen. 2016. "Tap Water Isotope Ratios Reflect Urban Water System Structure and Dynamics across a Semiarid Metropolitan Area." *Water Resources Research* 52: 5891–910. https://doi.org/10.1002/2016wr019104.

Jefferson, A.J., C.D. Bell, S.M. Clinton, and S.K. McMillan. 2015. "Application of Isotope Hydrograph Separation to Understand Contributions of Stormwater Control Measures to Urban Headwater Streams." *Hydrological Processes* 29 (25): 5290–306. https://doi.org/10.1002/hyp.10680.

Jensen, S.F., and N. Rees. 2005. *Jordan River Watershed Water Quality TMDL Assessment*. Salt Lake: State of Utah Division of Water Quality. http://slco.org/watershed/pdf/wqJrTMDL.pdf.

Kaushsal, S.S., P.M. Groffman, L.E. Band, E.M. Elliott, C.A. Shields, and C. Kendall. 2011. "Tracking Nonpoint Source Nitrogen Pollution in Human-Impacted Watersheds." *Environmental Science and Technology* 45 (19): 8225–32. https://doi.org/10.1021/es200779e.

Kendall, C., and E.A. Caldwell. 1998. "Fundamentals of Isotope Geochemistry." In *Isotope Tracers in Catchment Hydrology*, edited by C. Kendall and J.J. McDonnell, 51–86. Amsterdam: Elsevier Science.

Kendall, C., and T.B. Coplen. 2001. "Distribution of Oxygen-18 and Deuterium in River Waters across the United States." *Hydrological Processes* 15 (7): 1363–93. https://doi.org/10.1002/hyp.217.

Kendall, C., M.G. Sklash, and T.D. Bullen. 1995. "Isotope Tracers of Water and Solute Sources in Catchments." In *Solute Modelling in Catchment Systems*, edited by S.T. Trudgill, 261–303. New York, NY: John Wiley and Sons Ltd.

Kormos, P.R., D. Marks, J.P. McNamara, H.P. Marshall, A. Winstral, and A.N. Flores. 2014a. "Snow Distribution, Melt and Surface Water Inputs to the Soil in the Mountain Rain-Snow Transition Zone." *Journal of Hydrology* 519: 190–204. https://doi.org/10.1016/j.jhydrol.2014.06.051.

Kormos, P.R., D. Marks, C.J. Williams, H.P. Marshall, P. Aishlin, D.G. Chandler, and J.P. McNamara. 2014b. "Soil, Snow, Weather, and Sub-Surface Storage Data from a Mountain Catchment in the Rain-Snow Transition Zone." *Earth System Science Data Discussion* 6 (1): 165–73. https://doi.org/10.5194/essd-6-165-2014.

Krabbenhoft, D.P., C.J. Bowser, M.P. Anderson, and J.W. Valley. 1990. "Estimating Groundwater Exchange with Lakes: 1. The Stable Isotope Mass Balance Method." *Water Resources Research* 26 (10): 2445–53. https://doi.org/10.1029/WR026i010p02445.

Landwehr, J.M., T.B. Coplen, and D.W. Stewart. 2014. "Spatial, Seasonal, and Source Variability in the Stable Oxygen and Hydrogen Isotopic Composition of Tap Waters Throughout the USA." *Hydrological Processes* 28 (21): 5382–422. https://doi.org/10.1002/hyp.10004.

Ledford, S.H., and L.K. Lautz. 2015. "Floodplain Connection Buffers Seasonal Changes in Urban Stream Water Quality." *Hydrologic Processes* 29 (6): 1002–16. https://doi.org/0.1002/hyp.10210.

Locatelli, L., O. Mark, P. Steen, K. Arnbjerg-Nielsen, A. Deletic, M. Roldin, and P. John. 2017. "Hydrologic Impact of Urbanization with Extensive Stormwater Infiltration." *Journal of Hydrology* 544: 524–37. https://doi.org/10.1016/j.jhydrol.2016.11.030.

Navarro, A., and M. Carbonell. 2007. "Evaluation of Groundwater Contamination Beneath an Urban Environment: The Besòs River Basin (Barcelona, Spain)." *Journal of Environmental Management* 85 (2): 259–69. https://doi.org/10.1016/j.jenvman.2006.08.021.

O'Driscoll, M., S. Clinton, A. Jefferson, A. Manda, and S. McMillan. 2010. "Urbanization Effects on Watershed Hydrology and In-Stream Processes in the Southern United States." *Water* 2 (3): 605–48. https://doi.org/10.3390/w2030605.

Parnell, A. 2016. "simmr: A Stable Isotope Mixing Model." R Package Version 0.3. https://CRAN.R-project.org/package=simmr.

Pataki, D., M. Carreiro, J. Cherrier, N. Grulke, V. Jennings, S.A. Pincetl, R. Pouyat, T. Whitlow, and W. Zipperer. 2011. "Coupling Biogeochemical Cycles in Urban Environments: Ecosystem Services, Green Solutions, and Misconceptions." *Frontiers in Ecology and Environment* 9 (1): 27–36. https://doi.org/10.1890/090220.

Paul, M.J., and J.L. Meyer. 2001. "Streams in the Urban Landscape." *Annual Review of Ecology and Systematics* 32: 333–65. https://doi.org/10.1146/annurev.ecolsys.32.081501.114040.

Price, J.R., S.H. Ledford, M.O. Ryan, L. Toran, and C.M. Sales. 2018. "Wastewater Treatment Plant Effluent Introduces Recoverable Shifts in Microbial Community Composition in Receiving Streams." *Science of the Total Environment* 613–614: 1104–16. https://doi.org/10.1016/j.scitotenv.2017.09.162.

R Core Team. 2016. *R: A Language and Environment for Statistical Computing*. Vienna, Austria: R Foundation for Statistical Computing. https://www.R-project.org.

Rice, J., and P. Westerhoff. 2017. "High Levels of Endocrine Pollutants in US Streams During Low Flow Due to Insufficient Wastewater Dilution." *Nature Geoscience* 10: 587–91. https://doi.org/10.1038/ngeo2984.

Salt Lake County. 2017. "SLCo Watershed: Stream and Rain Gauging Program." Salt Lake County. https://rain-flow.slco.org/level.php.

Song, C., W.K. Dodds, J. Rüegg, A. Argerich, C.L. Baker, W.B. Bowden, M.M. Douglas et al. 2018. "Continental-Scale Decrease in Net Primary Productivity in Streams Due to Climate Warming." *Nature Geoscience* 11: 415–20. https://doi.org/10.1038/s41561-018-0125-5.

Thiros, S.A. 2003. "Quality and Sources of Shallow Ground Water in Areas of Recent Residential Development in Salt Lake Valley, Salt Lake County, Utah." *U.S. Geological Survey, Water-Resources Investigations Report 03-4028*. https://pubs.usgs.gov/wri/wri034028/.

Thiros, S.A., and A.H. Manning. 2004. "Quality and Sources of Ground Water Used for Public Supply in Salt Lake Valley, Salt Lake County, Utah, 2001." *U.S. Geological Survey, Water-Resources Investigations Report 03-4325*. https://pubs.water.usgs.gov/wri034325.

Tipple, B.J., Y. Jameel, T.H. Chau, C.J. Mancuso, G.J. Bowen, A. Dufour, L.A. Chesson, and J.R. Ehleringer. 2017. "Stable Hydrogen and Oxygen Isotopes of Tap Water Reveal Structure of the San Francisco Bay Area's Water System and Adjustments during a Major Drought." *Water Resources* 119: 212–24. https://doi.org/10.1016/j.watres.2017.04.022.

U.S. Census Bureau. 2016. "State and County QuickFacts." U.S. Census Bureau. https://www.census.gov/quickfacts/fact/table/US/PST045217.

U.S. Climate Data. 2017. "U.S. Climate Data: Temperature, Precipitation, Sunshine, Snowfall." U.S. Climate Data. http://www.usclimatedata.com/climate/salt-lake-city/utah/united-states/usut0225.

USGS (U.S. Geologic Survey). 2017. "USGS Current Water Data for the Nation." USGS Water Resources. https://waterdata.usgs.gov/nwis/rt.

UTDWQ (Utah Division of Water Quality). 2012. "Jordan River Total Maximum Daily Load Water Quality Study — Phase I. Prepared by Cirrus Ecological Solutions and Stantec Consulting. http://www.waterquality.utah.gov/TMDL/JORDAN/JordanRiverTMDL_Approved%20Document%20for%20EPA%209.26.2012.pdf.

UTDWR (Utah Division of Water Rights). 2018. "Real-Time Distribution System Information." Utah Division of Water Rights. https://waterrights.utah.gov/distinfo/realtime_info.asp.

van Vliet, M.T.H., M. Flörke, and Y. Wada. 2017. "Quality Matters for Water Scarcity." *Nature Geoscience* 10 (11): 800–02. https://doi.org/10.1038/ngeo3047.

Waswa, G., A.D. Clulow, C. Freese, P.A.L. Le Roux, and S.A. Lorentz. 2013. "Transient Pressure Waves in the Vadose Zone and the Rapid Water Table Response." *Vadose Zone Journal* 12 (1). https://doi.org/10.2136/vzj2012.0054.